Nanoscale

Accepted Manuscript

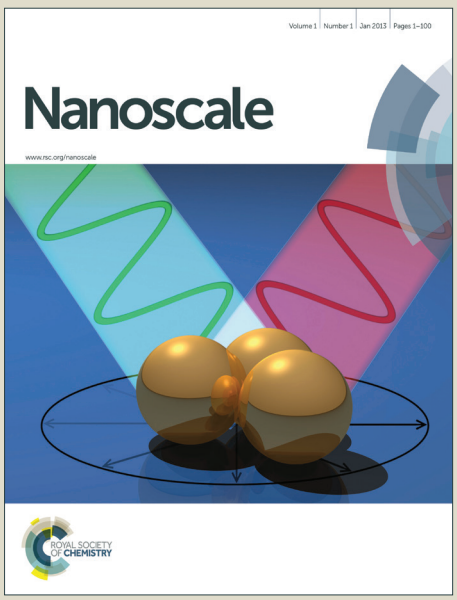

ROYAL SOCIETY OF CHEMISTRY

www.rsc.org/nanoscale

Nanoscale

ARTICLE

Novel stable dendrimersome formulation for safe bioimaging applications

Received 00th January 20xx,
Accepted 00th January 20xx

DOI: 10.1039/x0xx00000x

www.rsc.org/

M. Filippi,[a] D. Patrucco,[a] J. Martinelli,[b] M. Botta[b], P. Castro-Hartmann[c], L. Tei[b] and E. Terreno[a]

Dendrimersomes are nanosized vesicles constituted by amphiphilic Janus dendrimers (JDs), which have been recently proposed as innovative nanocarriers for biomedical applications. Recently, we have demonstrated that dendrimersomes self-assembled from (3,5)12G1-PE-BMPA-G2-$(OH)_8$ dendrimers can be successfully loaded with hydrophilic and amphiphilic imaging contrast agents. Here, we present two newly synthesized low generation isomeric JDs: JDG0G1(3,5) and JDG0G1(3,4). Though less branched than the above-cited dendrimers, they retain the ability to form self-assembled, almost monodisperse vesicular nanoparticles. This contribution reports on the characterization of such nanovesicles loaded with the clinically approved MRI probe Gadoteridol and the comparison with the related nanoparticles assembled from more branched dendrimers. Special emphasis was given to the *in vitro* stability test of the systems in biologically relevant media, complemented by preliminary *in vivo* data about blood circulation lifetime collected in healthy mice. The results point to very promising safety and stability profiles of the nanovesicles, in particular for those made of JDG0G1(3,5), whose spontaneous self-organization in water gives rise to an homogenous suspension. Importantly, the blood lifetimes of these systems are comparable to those of standard liposomes. By virtue of the reported results, the herein presented nanovesicles augur well for a future use in a variety of biomedical applications.

Introduction

The Biomimetic materials capable of reproducing the architecture and the properties of natural membranes are attracting much interest in the field of biomedical sciences.[1,2] Some natural or synthetic amphiphiles can simulate the behaviour of cell membrane components by self-assembling into organized structures when placed into aqueous environments.[3,4] Liposomes are the best-known example of artificial nanosized vesicles, and consist of a phospholipid bilayer entrapping an aqueous core.[5,6] They are successfully used for a number of biomedical purposes: from model systems to study biological membranes to efficient vectoring carriers for delivering bioactive substances or other molecules to pathological sites.[7-9] The need for systematic approaches to optimize specific membrane physico-chemical characteristics (e.g. mechanical resistance, wall thickness, chemical groups exposed on the outer surface) has driven the search for new categories of amphiphiles other than phospholipids.[10-12] Two examples are represented by polymersomes[13-15] and dendrimersomes,[16-22] which are obtained through the self-assembly of amphiphilic block co-polymers or Janus dendrimers (JDs), respectively. Whereas the potential of polymersomes in biomedical studies has been already demonstrated,[14,15] dendrimersomes have been proposed only very recently, and therefore their behaviour in biological environments is largely unexplored. A relevant exception are glycodendrimersomes, which were primarily proposed as nanotools to investigate specific protein functionalities (*e.g.* lectins), as well as the binding to biomolecules from plants and bacteria.[23-25]

We have recently reported that dendrimersomes assembled from (3,5)12G1-PE-BMPA-G2-$(OH)_8$ Janus dendrimer (herein coded as JDG1G2(3,5), **Figure 1**) can be loaded with both fluorescent and magnetic resonance imaging (MRI) contrast agents, thus potentially acting as a novel nanosized platform for molecular imaging applications.[26] Intriguingly, the encapsulation of the clinically approved MRI agent Gadoteridol (Figure 1) in the aqueous core of the dendrimersomes proved the high water permeability of their membrane with respect to clinically used liposomes.[27] Hence, the longitudinal relaxivity (r_1) of the paramagnetic agents encapsulated in the dendrimersomes (a measure of the ability to generate MRI contrast) is not severely limited by this parameter. Thanks to these distinctive features, JDG1G2(3,5)-based dendrimersomes possess a good diagnostic and theranostic potential.

[a] *Dipartimento di Biotecnologie Molecolari e Scienze della Salute, Centro di Imaging Molecolare e Preclinico, Università degli Studi di Torino, Via Nizza 52, Torino, 10126, Italia.*Corresponding author: E-mail: enzo.terreno@unito.it, Telephone: +39 011 6706452, Fax: +39 011 6706487.*
[b] *Dipartimento di Scienze ed Innovazione Tecnologica, Università del Piemonte Orientale "Amedeo Avogadro", Viale T. Michel 11, Alessandria, 15121, Italia.*Corresponding author: E-mail: lorenzo.tei@uniupo.it, Telephone: +39 0131 360 208, Fax: +39 0131 360250.*
[c] *Servei de Micorscòpia. Universitat Autònoma de Barcelona, 08193, Cerdanyola del Vallès, Spain.*
† Electronic Supplementary Information (ESI) available. See DOI: 10.1039/x0xx00000x

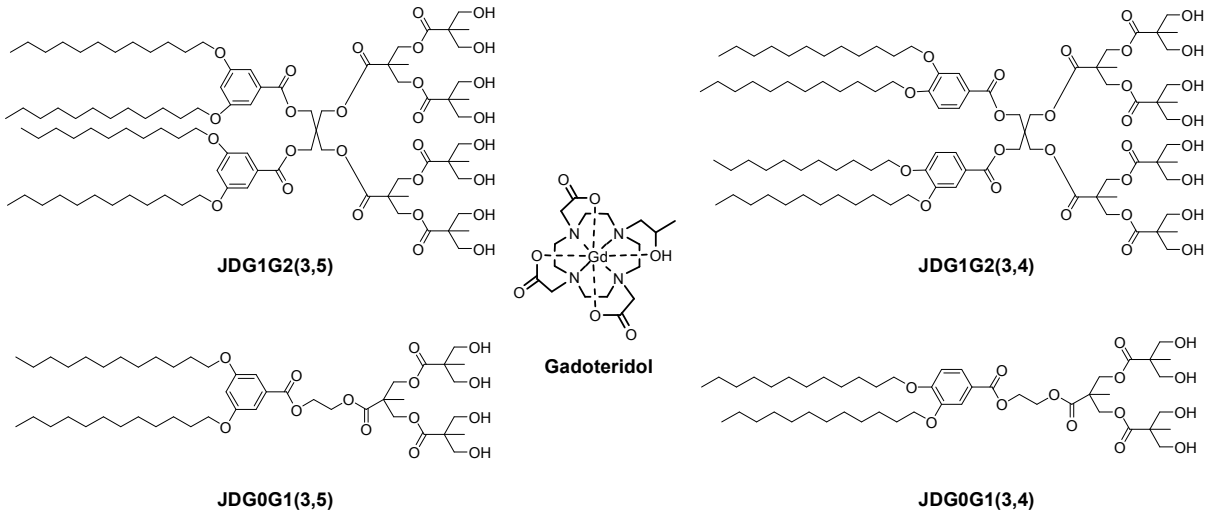

Figure 1. Chemical structures of Gadoteridol (in the centre) and of the Janus dendrimers investigated in this work: JDG1G2(3,5) (top left), JDG1G2(3,4) (top right), JDG0G1(3,5) (bottom left), JDG0G1(3,4) (bottom right).

In this contribution, two novel low-generation isomeric JDs (coded JDG0G1(3,4) and JDG0G1(3,5)) bearing only one hydrophobic and one hydrophilic dendron linked together by an ethylene glycol residue (Figure 1) have been synthesized. The ability of such dendrimers to form nanovesicles and to entrap Gadoteridol was assessed and compared with the results obtained with the higher generation dendrimersomes based on JDG1G2(3,4) and JDG1G2(3,5). For *in vivo* applications, the dendrimersomes were formulated with a small percentage of DSPE-PEG2000-COOH to increase stability and blood residence lifetime. For the first time, the structural integrity of this class of nanoparticles was tested in media mimicking the physico-chemical conditions of biological environments. Specifically, considerable effort was addressed to define the stability of vesicles in the presence of plasma components. In order to evaluate unexpected harmful effects on cell viability and proliferation, dendrimersomes were incubated in the presence of two distinct lines of murine macrophages (J774.A1 and RAW 264.7) and one murine fibroblast cell line (NIH/3T3). Finally, the vesicles were injected in healthy mice with the aim of assessing their blood circulation lifetime.

2. Results

2.1 Synthesis of JDs and their self-assembled dendrimersomes.

The novel amphiphiles JDG0G1(3,5) and JDG0G1(3,4) were properly designed to reduce the time required for the synthesis, and with the expectations to keep unaltered, or even improve, the physico-chemical properties of the resulting nanovesicles. Very recently, Percec and co-workers have reported a similar approach.[18] They called these molecules "single-single" amphiphilic Janus dendrimers, in contrast to the "twin-twin" homologous previously studied.[16] Such "single-single" JDs were obtained by using short mono/bis-amides or esters linkers connecting the hydrophilic and the hydrophobic moieties of the molecule. Our approach was somehow simpler, as we employed the same synthons used for the synthesis of low generation Janus dendrimers precursors of JDG1G2(3,5) and JDG1G2(3,4) that were connected through an ethylene glycol linker. In particular, as reported in **Scheme 1**, 2-hydroxyethyl 3,5-(didodecyloxy)benzoate (**1**) was obtained by reacting 3,5-(didodecyloxy)benzoic acid with an excess of

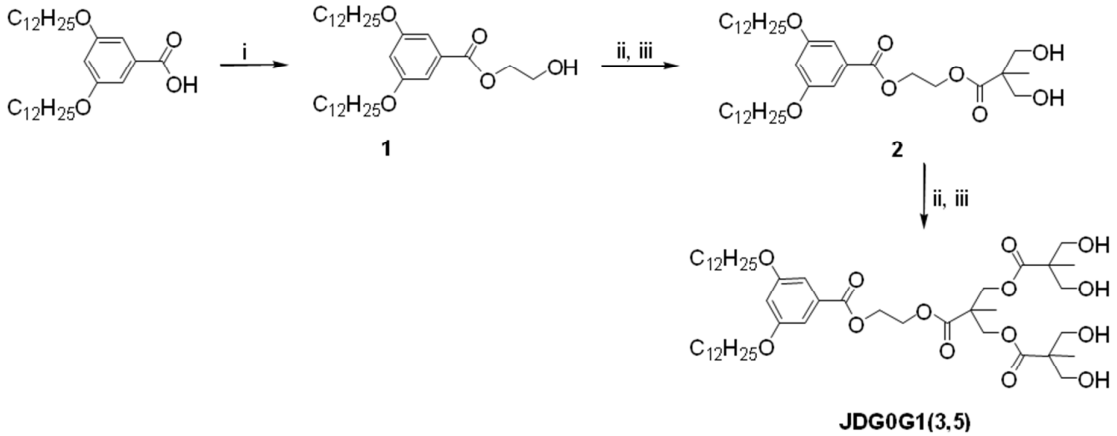

Scheme 1. Synthesis of JDG0G1(3,5) Janus dendrimer. i: ethylene glycol, DCC, DPTS; ii: 2,2,5-trimethyl-1,3-dioxane-5-carboxylic acid, DCC, DPTS; iii: THF, HCl 6M. The synthetic procedure is analogous for JDG0G1(3,4), starting from 3,4-(didodecyloxy)benzoic acid.

	Mean Diameter [nm]	PDI [a]	r_1 [b] [$s^{-1}mM^{-1}$]	P_w [c] [$\mu m\ s^{-1}$]
JDG1G2(3,5)	173.7 ± 15.9	0.15 ± 0.02	3.5 ± 0.2	146.5 ± 26.5
JDG1G2(3,4)	129.3 ± 5.2	0.20 ± 0.04	3.2 ± 0.2	170.3 ± 23.3
JDG0G1(3,5)	148.8 ± 6.4	0.13 ± 0.03	3.7 ± 0.2	139.4 ± 27.0
JDG0G1(3,4)	117.2 ± 9.9	0.18 ± 0.07	3.7 ± 0.1	148.9 ± 35.5

[a] Polydispersity Index; [b] Normalized longitudinal relaxivity r_1, calculated from the measurement of water protons longitudinal relaxation rate R_1^{obs} (20 MHz, 25°C); [c] Membrane water permeability.

Table 1. Physico-chemical properties of the investigated dendrimersomes.

ethylene glycol in the presence of 4-(dimethylamino)pyridinium *p*-toluenesulfonate (DPTS) and dicyclohexylcarbodiimide (DCC). Following the same coupling procedure, 2,2,5-trimethyl-1,3-dioxane-5-carboxylic acid was reacted with the free hydroxyl group of **1**. Deprotection of the acetonide was carried out in a 1:1 mixture of 6 M HCl and THF to get the generation zero intermediate **2**. The final compound JDG0G1(3,5) was obtained by repeating once again the coupling and the deprotection steps. The preparation of the analogous compound JDG0G1(3,4) was achieved starting from 3,4-(didodecyloxy)benzoic acid and following the same synthetic route (see ESI).

Dendrimersomes composed by the synthesized JDs (with 5% addition of DSPE-PEG2000-COOH) were prepared by using the conventional film hydration method. After extrusion and exhaustive dialysis, spherical vesicular structures with unilamellar membrane and homogeneous particle size distribution were obtained, as shown by cryo-transmission electron microscopy (Cryo-TEM) on selected systems (**Figure 2**) and Dynamic Light Scattering (DLS, **Table 1**). As previously reported,[16,17,20] the position of the aliphatic chains inside the branching pattern of the amphiphilic molecules may affect the membrane packing (Table 1 and Figure S1). As a consequence, the mean hydrodynamic diameter of vesicles made of 3,5-based JDs was found to be slightly larger than that of the 3,4-based dendrimersomes. This finding agrees with previous works reporting that the 3,5-positions can induce highly interdigitated wall architectures, resulting in larger vesicles.[16,17,20]

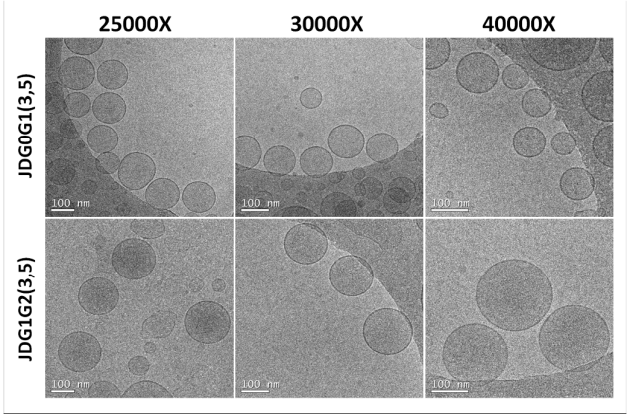

Figure 2. Cryo-TEM images of JDG0G1(3,5)-based and JDG1G2(3,5)-based dendrimersomes (top and bottom, respectively), at different magnifications (25000X, 30000X, 40000X), showing unilamellar vesicular architectures with homogeneous size distribution.

2.2 Relaxivity of dendrimersomes loaded with Gadoteridol

The normalized longitudinal proton relaxivity values r_1 (20 MHz, 25°C) of the MRI contrast agent Gadoteridol encapsulated in the G0G1-based dendrimersomes were only slightly lower (Table 1) than the value measured for the non-entrapped ("free") complex (4.6 $mM^{-1}s^{-1}$).[26] This result confirms that the membranes of these new dendrimersomes maintain a high water permeability, thus preventing the decrease of r_1 typically observed for the clinical-like formulations of liposomes.[27]

2.3 Dendrimersomes stability in vitro

The stability of the dendrimersomes was evaluated in terms of the release of the entrapped Gadoteridol after exhaustive dialysis, which was quantified by relaxometry. Stability tests were performed in: i) isotonic buffer at both 4 and 37°C; ii) human serum (HS) at 37°C; iii) human serum albumin (HSA) at 37°C. After 1 h of incubation in isotonic buffer at 4 or 37°C, followed by exhaustive dialysis, JDG0G1(3,4)-based dendrimersomes released most of their cargo, thus indicating some deficits in the basic stability or in the self-assembling process (Figures S2 and S3, ESI). The release of Gadoteridol from JDG0G1(3,4)-based vesicles was higher than from the dendrimersomes assembled from the other three JDs, even before dialysis.

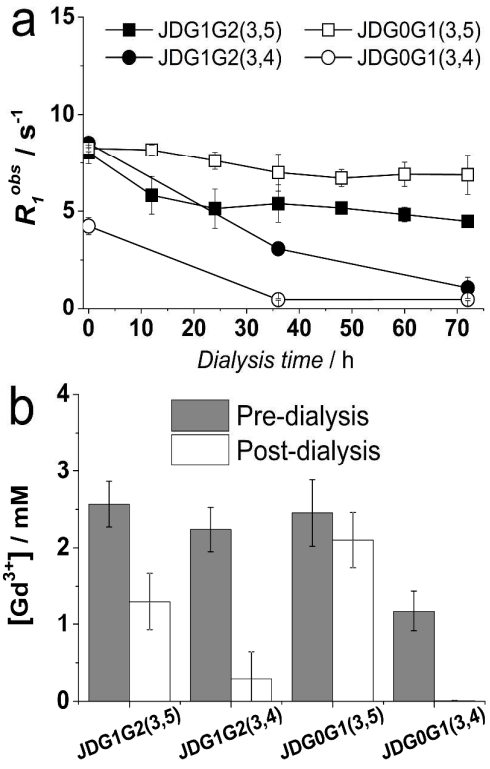

Figure 3. Stability and payload release in presence of human serum. a) Water protons longitudinal relaxation rate (R_1^{obs}) values measured for suspensions of dendrimersomes composed of different JDs incubated for 1 h in human serum at 37°C and successively dialyzed along consecutive time intervals (12 h each). b) Concentration of Gd^{3+} in the dendrimersome suspension before and after dialysis (6 cycles).

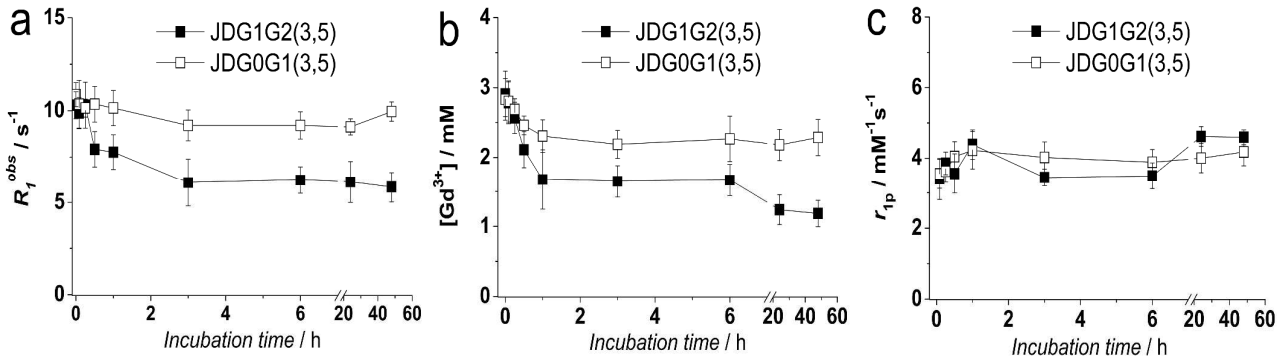

Figure 4. *In vitro* stability of (3,5)JD-based dendrimersomes in human serum. a) Water protons longitudinal relaxation rate (R_1^{obs}) of different suspensions of dendrimersomes in human serum (HS) as a function of the incubation time at 37 °C. R_1^{obs} was measured on the samples after dialysis. b) Residual concentration of Gd^{3+} in the sample, and c) normalized longitudinal relaxivity (r_1) at each time point.

This result suggests that the leakage of the MRI agents could have already started during the dialysis process that is included in the preparation protocol of the nanovesicles. When incubated with HS at 37°C, also dendrimersomes composed of JDG1G2(3,4) failed to retain their content (**Figure 3**).

Under the same conditions, JDG1G2(3,5) dendrimersomes showed a reduced and time-decreasing retention capability, while JDG0G1(3,5)-based vesicles displayed the highest stability. To investigate in more detail the effects caused by serum components on vesicular stability, additional release experiments were performed for the two most stable dendrimersomes based on (3,5)-substituted JDs. Unlike the previous experiments, the longitudinal water protons relaxation rate R_1^{obs} and the Gd^{3+} content were determined on dialyzed samples previously incubated in a given medium (buffer, HS or HSA) for different time intervals up to 6 hours. In isotonic buffer, no appreciable release was observed over 6 h (Figure S4). On the contrary, in HS some Gadoteridol was released already after very short incubation times (**Figure 4**). Payload releases of about 45% and 25% were detected after 1 h for dendrimersomes based on JDG1G2(3,5) and JDG0G1(3,5), respectively. Finally, the normalized r_1 values calculated at each time point remained constant and reproduced the expected values reported in Table 1, to indicate that no significant structural/dynamic variations occurred for the metal chelate entrapped in the nanovesicles.

Because serum albumin is the most abundant plasma protein,[28] its interaction with JDG0G1(3,5)-based nanovesicles was investigated. The results obtained (**Figure 5**) paralleled the data observed in HS.

PDI changes were observed after incubation with HS or HSA (**Figure 6**), suggesting that the interaction with plasmatic components may somehow destabilize the membrane of the vesicles.[29] In accordance with the data on Gadoteridol release, the PDI values of dendrimersomes suspensions increased just after the incubation with HS/HSA.

The loss of dimensional uniformity appeared to be more dramatic on JDG1G2(3,5)-based vesicles, which also displayed a higher Gadoteridol release under the same incubation conditions. We can tentatively hypothesize that a stronger affinity of the higher generation dendrimer towards the serum proteins might be responsible for the lower stability of the JDG1G2(3,5)-based vesicles in these media.

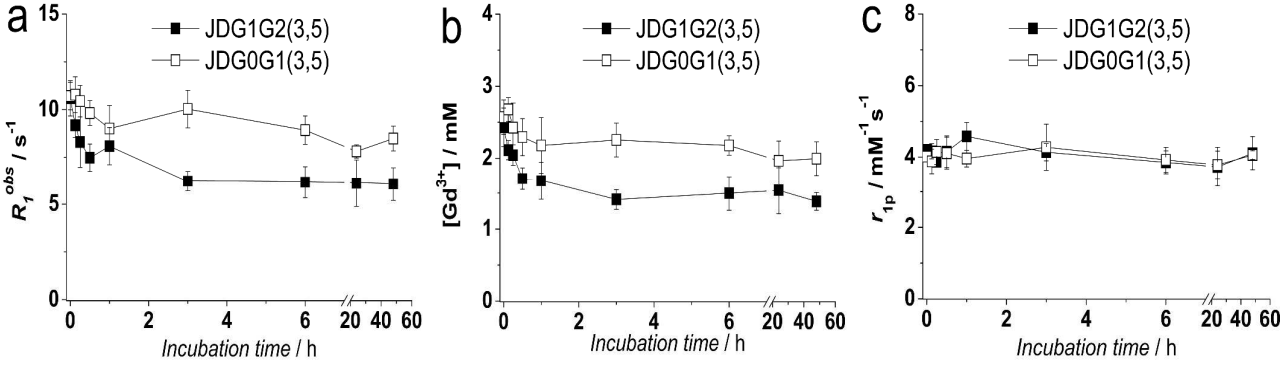

Figure 5. *In vitro* stability of (3,5)JD-based dendrimersomes in Human Serum Albumin. a) Water protons longitudinal relaxation rate (R_1^{obs}) of different suspensions of dendrimersomes in human serum albumin (HSA, 50 mg/ml) as a function of the incubation time at 37 °C. R_1^{obs} was measured on the samples after dialysis. b) Residual concentration of Gd^{3+} in the sample, and c) normalized longitudinal relaxivity (r_1) at each time point.

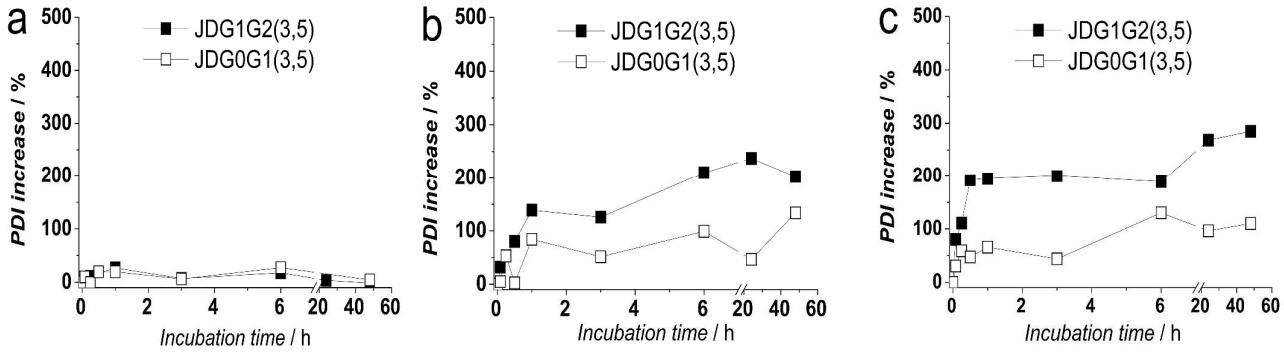

Figure 6. Changes in dimensional homogeneity. Percentage variation of the Polidispersity Index (PDI) of dendrimersomes as a function of incubation times at 37°C with a) isotonic buffer, b) Human Serum, and c) Human Serum Albumin.

Finally, JDG0G1(3,5)-based dendrimersomes presented a capability of payload retention similar to that of conventional formulation of liposomes (**Figure 7**). After incubation at different temperatures (4°C and 37°C) or in the presence of HSA, the Gadolinium(III) content in the suspensions was similar to the initial concentration for both dendrimersomes and liposomes. Nevertheless, as previously reported,[26] for all tested conditions the longitudinal relaxivity (r_{1p}) resulted to be higher for dendrimersomes due to the high water permeability of their membrane.

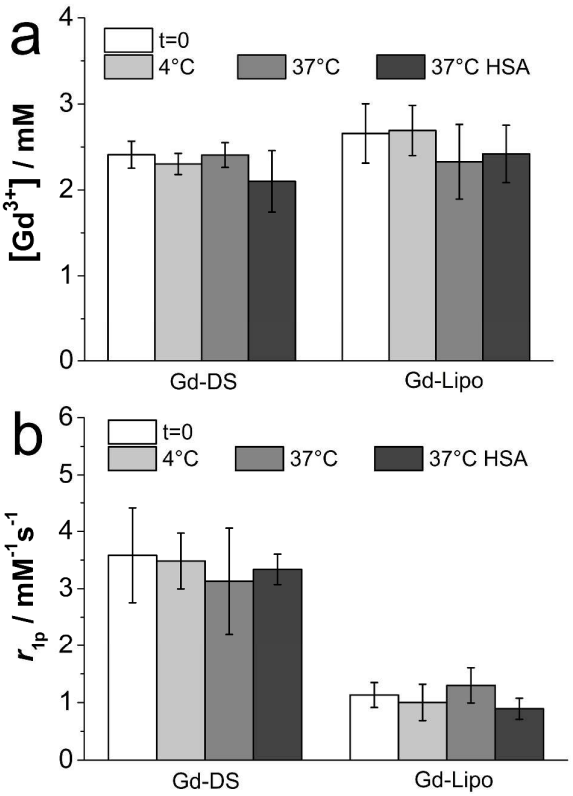

Figure 7. Stability and payload release of JDG0G1(3,5)-based dendrimersomes and standard liposomes. a) Concentration of Gd^{3+} measured for suspensions of JDG0G1(3,5)-based dendrimersomes (Gd-DS) and standard liposomes (Gd-Lipo) immediately after the preparation (t=0), after incubation for 1 h at 4°C, at 37°C and at 37°C in the presence of human serum albumin. b) Normalized longitudinal relaxivity (r_{1p}) calculated for the vesicular suspensions.

2.4 Cytotoxicity and cell proliferation

The more stable JDG0G1(3,5)-based dendrimersomes were further tested for their biocompatibility on two murine macrophage (RAW 264.7 and J774A.1) and one murine fibroblast (**Figure 8**, S5, and S6) cell lines. Cell viability was tested using Trypan Blue and Resazurin-Resofurin assays. Cells were incubated with the dendrimersomes at different concentrations ranging from 0.1 to 10 mg/ml of JDs. In Trypan Blue exclusion assay, both empty and Gadoteridol-containing vesicles were tested and in both cases the cell viability was found to be unaffected. Even longer incubation times (up to 48 hours) and the presence of highly concentrated dendrimersomes (10 mg/ml) did not influence cell viability. Furthermore, no significant differences were observed between vesicles encapsulating Gadoteridol or not, with cell viability matching the controls in both cases. Resazurin-Resofurin assays brought additional confirmation of these results, indicating that all tested cell lines retained active metabolism after 1 h exposure to Gadoteridol-loaded dendrimersomes. The proliferation rate of both cell lines was assessed after 1 h incubation with highly concentrated suspensions of dendrimersomes (**Figure 9**).

The nanovesicles did not affect cell proliferation, and no differences in growth kinetics were noticed for any tested material with respect to control incubation with PBS.

Similar data were collected also for JDG1G2(3,5)-based dendrimersomes, with no significant effects on cell viability and proliferation (Figure S7, S8, S9, and S10).

2.5 Blood circulation lifetime

JDG0G1(3,5) dendrimersomes loaded with Gadoteridol were i.v. injected in healthy BALB/c mice and the amount of circulating Gadolinium(III) was quantified by ICP-MS at different time points (until 24 h post-injection, **Figure 10**). The *in vivo* results were compared to those obtained for conventional liposomes prepared with a standard membrane formulation (containing the same pegylated component, DSPE-PEG2000-COOH), and to those observed by injecting an equivalent dose of free Gadoteridol. After the administration

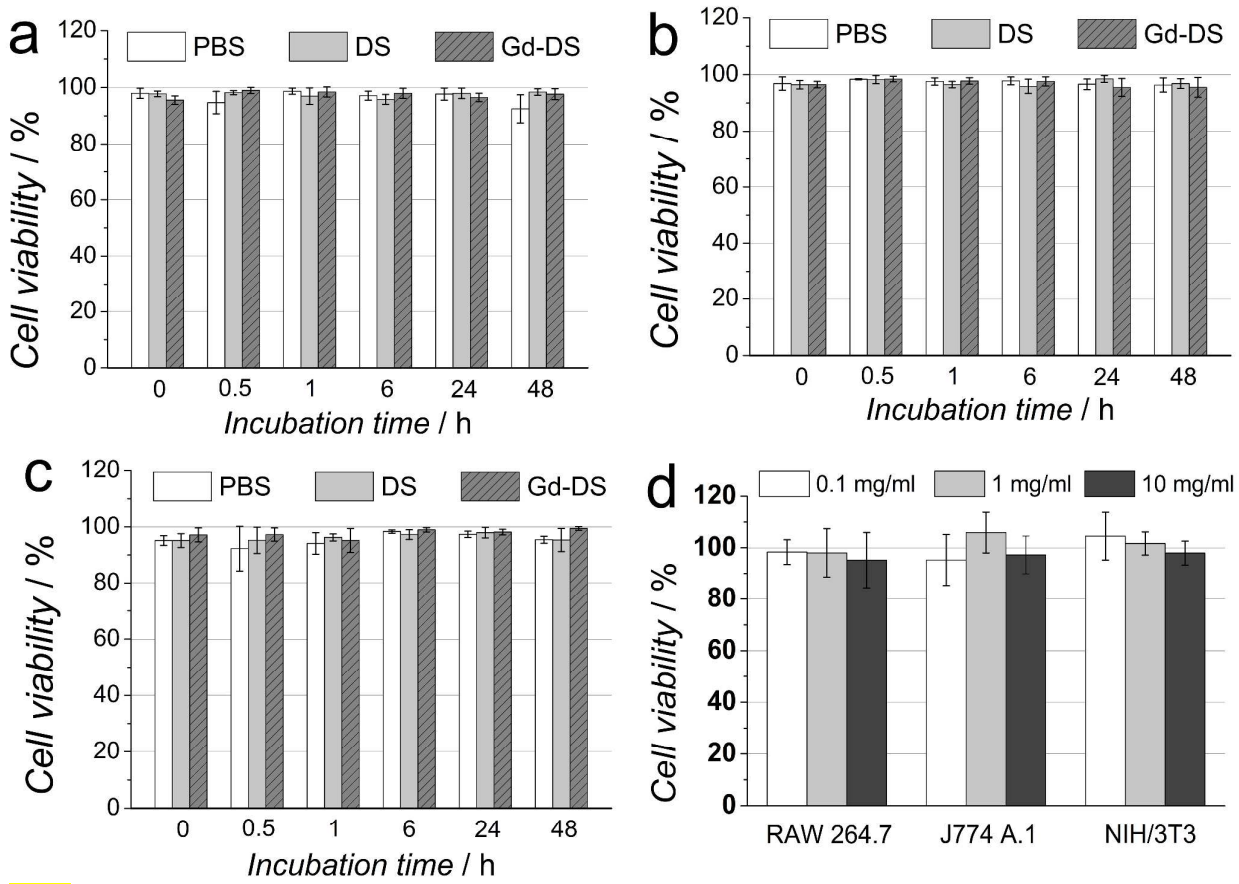

Figure 8. Effects of JDG0G1(3,5)-based dendrimersomes on cell viability. Cell viability estimated by Trypan Blue assay on a) RAW 264.7 cells, b) J774A.1 cells and c) NIH/3T3 cells after incubation along different incubation times with PBS or JDG0G1(3,5)-based vesicles at high concentration (10 mg/ml), encapsulating Gadoteridol or not (Gd-DS and DS respectively; d) cell viability estimated by Resazurin/Resofurin assay after 1 h incubation with JDG0G1(3,5)-based vesicles at different concentrations (0.1/1/10 mg/ml).

of dendrimersomes, the Gadolinium(III) content in mice blood progressively decreased, being completely eliminated from circulation within 24 h. A blood lifetime of 70-80 min could be extrapolated by a simple visual inspection of the data.

Liposomes showed a very similar trend. Interestingly, the amount of Gd^{3+} measured few minutes after injection was ca. 25% lower than the injected dose for both the nanovesicular systems, thus suggesting that the initial release of Gadoteridol observed *in vitro* may also occur *in vivo* with a much faster kinetic.

Nevertheless, the decrease in the plasmatic Gadoteridol concentration was even more rapid, confirming that the inclusion into both nano-sized carriers provides an advantageous clearance delay for *in vivo* use. Furthermore, a different biodistribution profile between Gadoteridol-loaded vesicles and free Gadoteridol was also proved by the tissue quantification of Gd(III) at 24 h post injection, revealing that dendrimersomes and liposomes accumulate in liver and

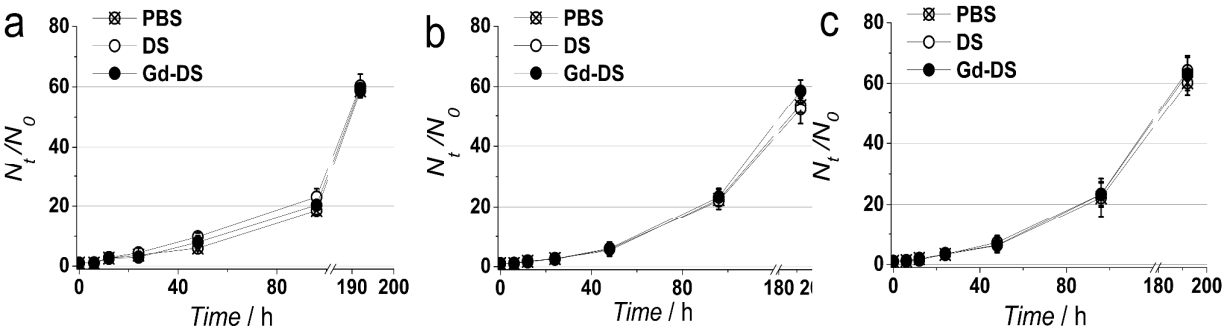

Figure 9. Effects of JDG0G1(3,5)-based dendrimersomes on cell proliferation. Proliferation rate of a) RAW 264.7 cells, b) J774A.1 cells and c) NIH/3T3 cells after 1 h incubation with PBS or JDG0G1(3,5)-based dendrimersomes (10 mg/ml of JD), loaded with Gadoteridol or not (Gd-DS and DS, respectively). N_t and N_0 represent the number of cells at each time point and the number of cells present at the beginning of the experiment respectively.

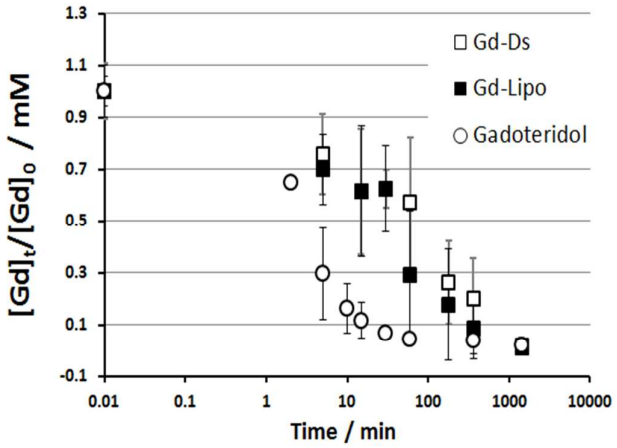

Figure 10. Blood circulation lifetime. Kinetics of gadolinium concentration in blood normalized to the injected dose ($[Gd]_t/[Gd]_0$) in healthy BALB/c mice after systemic injection of Gadoteridol (white circles), JDG0G1(3,5) dendrimersomes (Gd-DS, white squares, error bars in grey) and control liposomes (Gd-Lipo, black squares) both loaded with Gadoteridol. All animals received equivalent Gadoteridol doses (0.16 mmol/kg bw).

spleen *i.e.* the macrophage-rich organs commonly responsible for the blood removal of of nanoparticles (Figure S11, ESI).

3. Discussion

Research on nanocarriers is rising exponentially as innovative medical approaches require high specificity and efficiency in local delivery of molecules employed for therapy or diagnosis.[30] New nanoplatforms are continuously proposed in search for effective solutions to deliver high molecular payload to the biological target.[31] As far as *in vivo* diagnostic or theranostic imaging is concerned, nanomaterials are very useful, especially in the MRI field,[32,33] since the intrinsic low sensitivity of the technique requires a high payload of efficient contrast agent molecules to generate a locally detectable signal. We have recently proposed the use of paramagnetic nanovesicles formed by the self-assembling of Janus dendrimers as novel nanosized MRI contrast agents.[26] As for other nanovesicular systems,[34] also in dendrimersomes the paramagnetic contrast agent can be embedded in the membrane, entrapped in the aqueous core, or covalently attached to the membrane components giving rise to different relaxivity enhancements depending on the location of the MRI probe in the nanoparticle.[26] We also found that the dendrimeric bilayer is highly permeable to water,[26] thus allowing to obtain higher relaxivities and improving the MRI detection of the nanoparticles.

Although many of the recently proposed nanocarriers are designed as ideal constructs for drug delivery and non-invasive imaging, most of them failed when placed into complex biological systems.[35,36] One of the most frequent drawbacks is related to the loss of stability and uncontrolled release of loaded molecules.[37-39] Hence, this issue has to be carefully considered before devising biological uses. Additionally, since in liposomes high water permeability is very often associated with a poor stability of the nanovesicles and a limited retention of entrapped molecules, there is a further interest to check the behaviour of dendrimersomes.

As in most of the biomedical applications nanomaterials are systemically administered, the first biological medium to consider is blood.[40,41] A good prediction of the *in vivo* stability of nanoparticles can be obtained by studying the *in vitro* behaviour in plasma-mimicking fluids. Nano-objects encapsulating substances inside the internal compartments should be carefully tested for their stability, since undesirable release events have been already described for standard liposome formulations after their interaction with different plasmatic components.[40-45] Interestingly, in many cases the release appears to follow a two-phases time dependence, with a rapid release in the early phase after the injection, followed by a slower phase, likely associated with the biodistribution/excretion of the nanoparticle.[46-50] Despite the lack of a detailed description of the mechanisms driving this phenomenon, a number of hypotheses have been proposed, including lipoproteins-mediated lipids transfer and direct interaction with albumin or lipoproteins.[41,42,49]

Although detailed studies about the structural stability of dendrimersomes have already been reported,[16-20] these did not consider specifically and thoroughly the role of biological variables. For this reason, we considered important to devote efforts to assess the ability of Gadoteridol-loaded dendrimersomes to retain their payload in blood-like environment.

Peterca *et al.* have recently demonstrated the presence of a direct correlation between the molecular structure of the dendrimer and the morphology of the supramolecular assemblies.[17] Specifically, the geometric pattern of the hydrophobic branching moiety in JDs can represent a key factor for the layer thickness inside lamellar phases in bulk and in vesicular wall. Vesicles self-assembled from JDs with 3,5-bis(dodecyloxy)benzene hydrophobic groups were reported to be characterized by thinner walls, larger dimensions, and higher resistance to mechanical stress with respect to the 3,4-functionalized isomers. The explanation is to be found in the thicker interdigitation pattern arising from the more separated alkyl chains in the former JDs. Since wall packing density and vesicular architecture are also responsible for the mechanical properties of the particles, it is likely that dendrimersomes stability and the release of their content are related to this phenomenon. Larger dendrimersomes with thinner membrane were described as tougher and generally more stable in storage conditions.[17]

Consistently, in the present study, dendrimersomes based on JDs with the 3,5-pattern (JDG0G1(3,5) and JDG1G2(3,5)) displayed a greater ability to retain the transported material than vesicles made of the (3,4) analogues even in isotonic buffer at 4°C. Interestingly, the stability in HS and HSA of the dendrimersomes composed by JDG0G1(3,5) was higher than that of the vesicles previously reported, made of higher generation JDs. As already observed in several cases, the release of the payload is stimulated by the interaction of the particles with plasma proteins,[48-50] as demonstrated by the

increase in the polydispersity of the nanosystems that shows a good correlation with the release data. However, after a first release "burst" (about 25% after 1 h), the nanovesicles displayed an excellent stability and the amount of encapsulated Gadoteridol did not change within 2 days of incubation in HS at 37°C.

Another relevant finding of this work is the high biocompatibility displayed by JDG0G1(3,5)-based dendrimersomes. In fact, the particles (both empty and loaded with Gadoteridol) did not produce any negative effect on cell viability and proliferation rate, which augurs well for their use in biomedicine.

Moreover, for the first time dendrimersomes were tested on animals with the primary aim of determining their blood circulation lifetime, which is one of the most important properties for assessing the *in vivo* potential of a nanoparticle. Given the difficulty to compare biodistribution data *in vivo* because of the high number of variables involved, we decided to compare the blood kinetics of JDG0G1(3,5)-based nanovesicles with that of standard liposomes of similar size (146.4 nm) on the same animal model (BALB/C healthy male mice with the same age and weight), using the identical analytical technique (ICP-MS) for the determination of the blood concentration of Gd^{3+}. The data reported in Figure 10 indicated that the two nanosystems display very similar profiles. According to non-parametric independent statistic tests such as Kolmogorov-Smirnov and Mann-Whitney analyses, the difference between the two samples did not result statistically significant.

A blood lifetime of ca. 70-80 min can be extrapolated for both the nanosystems. However, it is worth noting that the amount of Gd^{3+} found in the blood five minutes after the injection of the nanovesicles was ca. 25-30 % lower than the total amount injected. This fraction closely corresponds to the amount of Gadoteridol released from the dendrimersomes *in vitro* after 1 h of incubation in the presence of HSA or HS (Figures 4 and 5). Likely, the mechanism(s) responsible for the "burst" release of Gadoteridol occurred *in vivo* on a much shorter timescale.

Interestingly, the confirmation of the initial fast release of Gadoteridol was achieved by measuring the blood kinetic of free Gadoteridol (Figure 10). In fact, the reduction of Gd(III) blood concentration few minutes after injecting the free complex was very similar to what determined for the nanovesicular form of the agent. Then, for longer times, the free complex was cleared faster, thus highlighting the prolonged circulation times of the Gd-loaded nanoparticles.

Considering such a very fast initial release, the actual blood lifetime of the nanoparticles related to their tissue/organ accumulation will be longer, around 90-120 min. This range of values has been already reported for stealth liposomes in healthy animals.[51,52]

Very importantly, during the *in vivo* experiments neither acute episodes of toxicity nor other side effects on general health conditions of animals were noticed, thereby indicating that dendrimersomes could effectively be employed in biological applications.

4. Experimental

Chemicals

The phospholipid 1,2-distearoyl-sn-glycero-3 phosphoethanolamine-N-[carboxy(polyethyleneglycol)-2000] ammonium salt (DSPE-PEG2000-COOH) and 1,2-dipalmitoyl-sn-glycero-3-phosphocholine (DPPC) were purchased from Avanti Polar Lipids Inc. (Alabaster, AL, USA). Gadoteridol (Gd-HPDO3A, marketed as ProHance™) was kindly provided by Bracco Imaging S.p.A. (Colleretto Giacosa, Torino, Italy). All other chemicals and reagents were purchased from Sigma-Aldrich (St. Louis, USA), and used as received except where noted otherwise.

Animals

Healthy male BALB/c mice involved in the study were obtained from Charles River Laboratories (Calco (LC), Italy) and maintained in standard housing conditions, with water and standard rodent chow ad libitum and 12 h light/dark cycle. Animal manipulation and all experimental procedures were performed in accordance with the European Community guidelines and approved by the Ethical Committee of University of Torino.

Synthesis of Janus dendrimers

The synthesis and characterization of (3,4)12G1-PE-BMPA-G2-$(OH)_8$ and (3,5)12G1-PE-BMPA-G2-$(OH)_8$ Janus dendrimers (JDG1G2(3,4) and JDG1G2(3,5) in Figure 1) was performed as described elsewhere.[16,17,53] The synthesis of JDG0G1(3,4) and JDG0G1(3,5) is described in detail in the Supplementary Materials. Briefly, the new amphiphiles were obtained by linking by means of an ethylene glycol spacer one hydrophobic block (3,4 or 3,5 bis-dodecyl substituted benzoyl ether) to a generation 1 BPMA-based hydrophilic moiety (BPMA: 2,2-bis(hydroxymethyl)propanoic acid).

Dendrimersome preparation

Dendrimersomes were prepared by thin film hydration method.[54] Briefly, appropriate amounts of JDs and DSPE-PEG2000-COOH (molar ratio of 95:5) were dissolved into chloroform. The organic solvent was slowly removed with a rotary evaporator, letting the amphiphilic components distributed in a thin homogeneous film. After two hours under vacuum, the films were hydrated at 50°C with an isotonic buffered HEPES solution (pH 7.4) containing 250 mM Gadoteridol. The samples were then extruded through polycarbonate filters (Lipex extruder, Northern Lipids Inc.) with pore diameters decreasing from 1 µm to 200 nm. After the extrusion process, the final suspensions underwent an exhaustive dialysis process against isotonic buffer at 4°C to remove the non-encapsulated agent. Dynamic Light Scattering (DLS) measurements allowed the determination of the mean hydrodynamic diameter of the vesicles and their polydispersity index (PDI). The value of the membrane water permeability of the dendrimersomes was determined relaxometrically.[55] Further details about the vesicles preparation and characterization are available in the ESI.

Cryo-TEM

Vitrified specimens were prepared by placing 3 µl of a sample on a Quantifoil® 1.2/1.3 TEM grid. Each sample was blotted to a thin film and immediately plunged into liquid ethane in the Leica EM CPC cryoworkstation. The grids were transferred to a 626 Gatan cryoholder and maintained at -179°C during imaging. The grids were studied on a JEOL 2011 transmission electron microscope operating at an accelerating voltage of 200 kV. Micrographs were recorded on a Gatan Ultrascan cooled charge-coupled device (CCD) camera under low electron dose conditions to minimize electron bean radiation.

In vitro stability

In order to test the stability within a biological environment, dendrimersomes loaded with Gadoteridol were incubated with isotonic solutions of plasma components at pH 7.4 and 37°C. The stability was evaluated by measuring the amount of released Gadoteridol by relaxometry (water proton longitudinal relaxation rate R_1^{obs} measurements). Vesicular suspensions (10 mg/ml of amphiphilic material) were diluted (ratio 1:2) with Human Serum Albumin (HSA, 50 mg/ml) or Human Serum (HS, SERO, Billingstad, Norway) and kept at 37°C for the required incubation time. Control tests were carried out by incubating the vesicles in isotonic HEPES buffer at 4°C or 37°C. The MRI agent released from the vesicles during the incubation was removed by dialysis at 4°C (6 h, receiving phase/donor phase volume > 1500).

In a first set of experiments, dendrimersomes were incubated for 1 h. Then, a prolonged dialysis was carried out at 4°C with recursive buffer renewals to completely wash out the non-encapsulated agent. The amount of gadolinium in the samples was assessed before and after the dialysis, while the observed water proton longitudinal relaxation rate R_1^{obs} was measured at each buffer renewal.

In a second set of experiments, an aliquot of the incubated sample was taken at each time point and subjected to a 6 h dialysis cycle at 4°C. After that, gadolinium content in the suspension and R_1^{obs} of the sample were measured.

In order to evaluate size and/or polydispersity changes occurring to the dendrimersomes, some aliquots of the samples incubated at 37°C with buffer, HSA or HS, were collected to be tested by DLS. Since DLS measurements can be severely affected by the presence of proteins, samples incubated with HSA or HS were dialyzed using membranes with a 100 kDa molecular weight cut-off, which permit the transit of proteins, but prevent the passage of the much bigger nanoparticles.

In a third set of experiments, the stability, the payload release and the contrast properties of dendrimersomes were compared to those observed for liposomes. For control liposomes, a standard membrane formulation was chosen (DPPC and DSPE-PEG2000-COOH in molar ratio 19:1). The normalized longitudinal relaxivity (r_{1p}) and the Gadolinium(III) content of vesicular suspensions were calculated (as explained in the following paragraphs) on the samples immediately after the preparation, or after a 1 h incubation at 4°C, at 37°C and at 37°C in presence of HSA.

See ESI for additional information about the stability experiments performed.

^{1}H NMR relaxation measurements

Observed water protons longitudinal relaxation rate (R_1^{obs}) values were measured on a Stelar SpinMaster Spectrometer (Stelar Snc, Mede (PV), Italy) operating at 20 MHz by using the standard inversion recovery pulse sequence with 4 scans for each acquired data point. A precise control of the temperature was operated during the measurements by means of a Stelar VTC-91 airflow heater equipped with a calibrated copper constantan thermocouple (uncertainty of ±0.1°C). Furthermore, the actual temperature inside the probe head was additionally monitored by a Fluke 52 k/j digital thermometer (Fluke, Zürich, Switzerland). The concentration of Gd^{3+} in the samples was determined by a relaxometric procedure (at 20 MHz) after mineralization. Briefly, the samples were diluted 1:2 into concentrated HCl (37%) and stored overnight at high temperature (120°C) in a sealed glass ampoule, to effectively remove the metal ions from the complexes and to obtain a solution containing free Gd^{3+} under the form of aqua-ion. The R_1^{obs} measurement (at 25°C) allowed for the accurate estimation of the Gd^{3+} concentration through a calibration line obtained by using standard solutions of $GdCl_3$.[56]

Cells

All cell lines were obtained from American Type Culture Collection (ATCC, Manassas, VA, USA) and resulted negative for mycoplasma test (MycoAlert™ Mycoplasma Detection Kit, Lonza Sales AG, Verviers, Belgium). Murine macrophages (J774A.1 and RAW 264.7 cell lines) and fibroblasts (NIH/3T3) were cultured as monolayers at 37°C in a 5% CO_2-containing humidified atmosphere in Dulbecco's modified Eagle's medium (DMEM). The medium was supplemented with 10% (v/v) of heat-inactivated fetal bovine serum, 2 mM of Glutamine, 100 U/ml of penicillin and 100 µg/ml of streptomycin.

When cells reached confluence, the detachment was accomplished by mechanical removal by means of a scraper (macrophages) or by trypsin addition (fibroblasts). All cells employed for cellular tests were at passages included between 3 and 7. Culture medium, fetal bovine serum, penicillin-streptomycin mixture and trypsin were all purchased from Lonza (Lonza Sales AG, Verviers, Belgium).

Cell viability and proliferation

To assess the cellular viability after the incubation with the dendrimersomes, $5x10^4$ RAW 264.7, J774A.1 or NIH/3T3 cells were plated in culture dishes. After 24 h, cells were added with dendrimersomes (previously diluted into culture medium and filtered by sterile 0.2 µm sized filters) at different incubation times (up to 2 days), and particles concentration (0.1, 1, and 10 mg/ml of JDs). Viable cells were counted by Trypan Blue exclusion assay: a 0.4% solution of Trypan Blue in Phosphate

Buffered Saline (pH 7.2-7.3; 1:1 v/v) was added to harvested cells before counting. Cells added with neat-buffered solution were used as control. Each incubation experiment was replicated eight times, and the reported cell viability percentage value represents the average ratio between the number of vital cells and the total number of cells counted in each experiment (*i.e.* $N_v/N_t * 100$).

In order to confirm the results obtained by Trypan Blue exclusion assay, dendrimersome cytotoxicity was further investigated by means of a fluorimetric cell viability assay, based on the cell metabolic activity (CellTiter-Blue® Cell Viability assay, Promega, Madison, USA). The CellTiter-Blue® reagent contains the indicator dye Resazurin that is reduced to highly fluorescent Resofurin by viable cells retaining metabolic capacities, so that the fluorescent signal generated from the assay is proportional to the number of living cells in the sample. Briefly, J774A.1, RAW 264.7 and NIH/3T3 cells were plated in 96-well multiwall plate at a concentration of 1.0×10^4, 1.5×10^4 and 1.0×10^4 cells per well, respectively. After 24 h, cells were exposed to fresh medium containing Gadoteridol-loaded dendrimersomes. After 1 h of incubation, the incubation medium was removed and wells were washed three times with sterile PBS. Then, the CellTiter-Blue® reagent was added following manufacturer's instructions (20 µl of reagent diluted 1:5 into culture medium for each well). After 4 h, supernatants were collected and placed in a black 96-well multiwell plate for fluorescence detection (excitation wavelength 530-560 nm, emission wavelength 590 nm). For each condition, six independent experiments were performed in triplicate and fluorescence measurements were repeated three times. Results are expressed as the mean ± SD of the percentage of viable cells, normalized with respect to control samples obtained by incubating cells with PBS-containing medium.

Proliferation tests were performed by incubating cells with dendrimersomes (10 mg/ml of JDs in culture medium) for 1 h. Then, cells were seeded in round plastic dishes and maintained in fresh culture medium for different time ranges (up to 7 days). Cells were then detached, collected, and counted by Trypan Blue assay at each time point. Each experiment was replicated five times. Cell proliferation was expressed as the ratio between the number of viable cells at each time point and the number of cells present at the beginning of the experiment (*i.e.* N_t/N_0).

In vivo stability

In vivo stability was investigated by injecting dendrimersomes *via* tail vein in healthy male BALB/c mice (8 weeks, 24-25 g). Each experiment was performed at least on three different animals. Gadoteridol-loaded dendrimersomes and liposomes (40 mg/ml of phospholipids) were relaxometrically analysed for their Gd^{3+} content and animals were administered to receive the same dose of Gd^{III} (0.16 mmol/kg). A standard membrane formulation was chosen for liposomes consisting of DPPC and DSPE-PEG2000-COOH in molar ratio 19:1. The results obtained for the two nanosystems were further compared to the in vivo kinetics of the free Gadoteridol at equivalent dose. After the injection, blood was sampled at different times up to 24 h, to measure the amount of circulating Gd^{III}. Animals were then sacrificed to obtain the organs (liver, spleen, kidneys, muscle, heart, lung) and to quantify the tissue metal concentration (see ESI for further details). The metal quantification was performed by ICP-MS measurement, after all biological specimens were completely digested into acid. Briefly, collected blood was immediately added to heparin (20 µL, Sigma-Aldrich, St. Louis, USA) and its volume was accurately measured. Each sample was treated with concentrated HNO_3 (70%) and digested by applying microwave heating (Milestone MicroSYNTH, Microwave labstation equipped with an optical fiber temperature control and HPR-1000/6M six position high-pressure reactor, Bergamo, Italy). After digestion, the remaining material was diluted in ultrapure water (final volume of 3 mL) and further filtered with 0.2 µm filters. Finally, samples were analysed by ICP-MS (Thermo Scientific ELEMENT 2 ICP-MS -Finnigan, Rodano, Milano, Italy) to measure the Gd^{3+} content. These values were finally reported as metal concentration values in blood by calculating the Total Blood Volume (TBV) for each animal from the average value reported for mice (79 ml/kg).[57]

5. Conclusions

In the present work, we report on the synthesis of new low-generation Janus dendrimers through a simplified synthetic pathway. In aqueous media, these amphiphiles spontaneously form nanovesicular dendrimersomes with size and PDI similar to higher generation JDs. The nanovesicles were loaded with the clinically approved MRI contrast agent Gadoteridol and ^1H NMR relaxometric measurements confirmed the high water permeability of the membrane of the new dendrimersomes, in analogy to their higher generation analogues. The payload stability of the nanovesicles was tested for the first time in human serum. The data indicate that one of the newly synthesized JDs (JDG0G1(3,5)) forms dendrimersomes with a higher stability than its higher generation precursor, as only a small percentage (ca. 25%) of Gadoteridol was released in the presence of serum.

In addition, these novel vesicles displayed a very high biocompatibility and no negative effects on cell viability and proliferation rate were observed on fibroblasts and on two populations of murine macrophages. Furthermore, pegylated dendrimersomes demonstrated to remain in blood vessels and to circulate for time periods comparable to those of conventional liposomes with similar size, that represent a well established tool for several biomedical applications.

Overall, these promising results suggest that JDG0G1(3,5)-based dendrimersomes are good candidates for the development of effective nanosystems for medical bioimaging. Future work will be directed to test the diagnostic/therapeutic/theranostic potential of this new class of soft nanoparticles at preclinical level.

Acknowledgements

The financial support of the ''Compagnia di San Paolo'' (CSP-2012 NANOPROGLY and ''Validazione di molecole di tipo VHH e Aptameri per il rilascio tumore-specifico di farmaci e la valutazione contestuale della risposta mediante imaging funzionale mirato'' projects), University of Torino (Innovative Nanosized Theranostic Agents) and European Union's FP7/2007–2013 under grant agreement no. HEALTH-F2-2011-278850 (INMiND) is gratefully acknowledged. This work was carried out within the framework of the COST TD1004 Action and of the Consorzio Interuniversitario di Ricerca in Chimica dei Metalli nei Sistemi Biologici (*C.I.R.C.M.S.B.*).

Notes and references

1 B. Zhu, J. Li and D. Xu, *Phys. Chem. Chem. Phys.,* 2011, **13**, 10584.
2 E. Reimhult, M. Baumann, S. Kaufmann, K. Kumar and P. Spycher, *Biotechnol. Genet. Eng. Rev.*, 2010, **27**, 185.
3 S.K.Mehta, S. Sharma, N. Mehta and S.S. Cameotra, *Adv. Exp. Med. Biol.*, 2010, **672,** 102.
4 M. Kwak and A. Herrmann, *Chem Soc Rev,* 2011, **40**, 5745.
5 J.C. Kraft, J.P. Freeling, Z. Wang and R.J. Ho, *J. Pharm. Sci.*, 2014, **103**, 29.
6 S. Mallick and J.S. Choi, *J. Nanosci. Nanotechnol.*, 2014, **14**, 755.
7 E. Sezgin and P. Schwille, *Mol. Membr. Biol.,* 2012, **29**, 144.
8 H. Daraee, A. Etemadi, M. Kouhi, S. Alimirzalu and A. Akbarzadeh, *Artif. Cells, Nanomed., Biotechnol.*, 2014, **15***,* 1.
9 N. Monteiro, A. Martins, R.L. Reis, N.M. Neves, *J. R. Soc. Interface,* 2014, **11**, 20140459.
10 G. Verma and P.A. Hassan, *Phys. Chem. Chem. Phys.,* 2015, **15**, 17016.
11 C. Wang, Z. Wang and X. Zhang. *Acc. Chem. Res.* 2012, **45**, 608.
12 Q. Meng, Y. Kou, X. Ma, Y. Liang, L. Guo, C. Ni and K. Liu. *Langmuir,* 2012, **28**, 5017.
13 D.E. Discher and A. Eisenberg, *Science,* 2002, **297**, 967.
14 P. Tanner, P. Baumann, R. Enea, O. Onaca, C. Palivan and W. Meier, *Acc. Chem. Res.,* 2011, **44**, 1039.
15 J. Nicolas, S. Mura, D. Brambilla, N. Mackiewicz and P. Couvreur, *Chem. Soc. Rev.,* 2013, **42**, 1147.
16 V. Percec, D. A. Wilson, P. Leowanawat, C. J. Wilson, A. D. Hughes, M. S. Kaucher, D. A. Hammer, D. H. Levine, A. J. Kim, F. S. Bates, K. P. Davis KP, T. P. Lodge, M. L. Klein, R. H. DeVane, E. Aqad, B. M. Rosen, A. O. Argintaru, M. J. Sienkowska, K. Rissanen, S. Nummelin and J. Ropponen, *Science,* 2010, **328**, 1009.
17 M. Peterca, V. Percec, P. Leowanawat and A. Bertin, *J. Am. Chem. Soc*., 2011, **133**, 20507.
18 S. Zhang, H. J. Sun, A. D. Hughes, B. Draghici, J. Lejnieks, P. Leowanawat, A. Bertin, L. Otero De Leon, O. V. Kulikov, Y. Chen, D. J. Pochan, P. A. Heiney, V. Percec, *ACS Nano,* 2014, **8**, 1554.
19 S. Zhang, H. J. Sun, A. D. Hughes, R. O. Moussodia, A. Bertin A, Y. Chen, D. J. Pochan, P. A. Heiney, M. L. Klein and V. Percec, *Proc. Natl. Acad. Sci. U .S. A.,* 2014, **111**, 9058.
20 H. J. Sun, S. Zhang and V. Percec, *Chem. Soc. Rev.,* 2014, **44**, 3900.
21 M. Giustini, C. Bellinazzo, L. Galantini, A. Mallardi, G. Palazzo, S. Sennato, F. Bordi and K. Rissanen, *Colloids Surf.*, 2012, **413**, 38.
22 X. Liu, J. Zhou, T. Yu, C. Chen, Q. Cheng, K. Sengupta, Y. Huang, H. Li, C. Liu, Y. Wang, P. Posocco, M. Wang, Q. Cui, S. Giorgio, M. Fermeglia, F. Qu, S. Pricl, Y. Shi, Z. Liang, P. Rocchi, J.J. Rossi and L. Peng, *Angew. Chem. Int. Ed*., 2014**,** **126**, 12016.
23 V. Percec, P. Leowanawat, H. J. Sun, O. Kulikov, C. D. Nusbaum, T. M. Tran, A. Bertin, D. A. Wilson, M. Peterca, S. Zhang, N. P. Kamat, K. Vargo, D. Moock, E. D. Johnston, D. A. Hammer, D. J. Pochan, Y. Chen, Y. M. Chabre, T. C. Shiao, M. Bergeron-Brlek, S. André, R. Roy, H. J. Gabius and P. A. Heiney, *J. Am. Chem. Soc.,* 2013, **135**, 9055.
24 S. Zhang, R.-O. Moussodia, H. J. Sun, P. Leowanawat, A. Muncan, C. D. Nusbaum, K. M. Chelling, P. A. Heiney, M. L. Klein, S. André, R. Roy, H. J. Gabius and V. Percec, *Angew. Chem. Int. Ed. Engl*., 2014, **53**, 10899.
25 S. Zhang, R.-O. Moussodia, C. Murzeau, H.-J. Sun, M. L. Klein, S. Vértesy, S. André, R. Roy, H. J. Gabius and V. Percec, *Angew. Chem. Int. Ed. Engl*., 2015, **54**, 4036.
26 M. Filippi, J. Martinelli, G. Mulas, M. Ferraretto, E. Teirlinck, M. Botta and E. Terreno, *Chem. Commun. (Camb),* 2014, **50**, 3453.
27 S. L. Fossheim, A. K. Fahlvik, J. Klaveness and R. N. Muller, *Magn. Reson. Imaging,* 1999, **17**, 83.
28 A. M. Merlot, D. S. Kalinowski and D. R. Richardson, *Front. Physiol*., 2014, **5**, 299.
29 K. Mohr, S. S. Müller, L. K. Müller, K. Rusitzka, S. Gietzen, H. Frey and M. Schmidt, *Langmuir,* 2014, **30**, 14954.
30 S. Marrache, R. K. Pathak, K. L. Darley, J. H. Choi, D. Zaver, N. Kolishetti and S. Dhar, *Curr. Med. Chem.,* 2013, **20**, 3500.
31 J. Ogier, T. Arnauld and E. Doris*, Future Med. Chem*., 2009, **1**, 693.
32 M. Ryvolova, J. Chomoucka, J. Drbohlavova, P. Kopel , P. Babula, D. Hynek, V. Adam, T. Eckschlager, J. Hubalek, M. Stiborova, J. Kaiser and R. Kizek, *Sensors*, 2012, **12**, 14792.
33 C. Felton, A. Karmakar, Y. Gartia, P. Ramidi, A. S. Biris and A. Ghosh, *Drug Metab. Rev.,* 2014, **46**, 142.
34 W. J. Mulder, G. J. Strijkers, G. A. Van Tilborg, A. W. Griffioen and K. Nicolay, *NMR Biomed.,* 2006, **19**, 142.
35 K. R. Vega-Villa, J. K. Takemoto, J. A. Yáñez, C. M. Remsberg, M. L. Forrest and N. M. Davies, *Adv. Drug. Deliv. Rev.,* 2008, **60**, 929.
36 Q. Sun, M. Radosz and Y. Shen, *J. Control. Release,* 2012, **164**, 156.
37 I. V. Zhigaltsev, N. Maurer, Q. F. Akhong, R. Leone, E. Leng, J. Wang, S. C. Semple and P. R. Cullis, *J. Control. Release,* 2005, **104**, 103.
38 E. Maurer-Spurej, K. F. Wong, N. Maurer, D. B. Fenske and P. R. Cullis, *Biochim. Biophys. Acta,* 1999, **1416**, 1.
39 C. Boyer and J. A. Zasadzinski, *ACS Nano*, 2007, **1**, 176.
40 C. A. Hunt*, Biochim. Biophys. Acta,* 1982, **719**, 450.
41 F. Bonté and R. L. Juliano, *Chem. Phys. Lipids,* 1986, **40**, 359.
42 L. S. Guo, R. L. Hamilton, J. Goerke, J. N. Weinstein and R. J. Havel, *J. Lipid. Res*., 1980, **21**, 993.
43 T. Hernández-Caselles, J. Villalaín and J. C. Gómez-Fernández, *Mol. Cell. Biochem*., 1993, **120**, 119.
44 K. Buyens, S. C. De Smedt, K. Braeckmans, J. Demeester, L. Peeters, L. A. van Grunsven, X. de Mollerat du Jeu, R. Sawant, V. Torchilin, K. Farkasova, M. Ogris and N. N. Sanders, *J. Control. Release,* 2012, **158**, 362.
45 V. Reshetov, V. Zorin, A. Siupa, M. A. D'Hallewin, F. Guillemin and L. Bezdetnaya, *Photochem. Photobiol.,* 2012, **88**, 1256.
46 L. Zeng, L. An and X. Wu, *J. Drug Deliv*., **2011**, 2011:370308, doi: 10.1155/2011/370308.
47 M. Hossann, M. Wiggenhorn, A. Schwerdt, K. Wachholz, N. Teichert, H. Eibl, R. D. Issels and L. H. Lindner, *Biochim. Biophys. Acta,* 2007, **1768**, 2491.
48 M. H. Gaber, K. Hong, S. K. Huang, D. Papahadjopoulos, *Pharm. Res.,* 1995, **12**, 1407.

49 T. M. Allen and L. G. Cleland, *Biochim. Biophys. Acta,* 1980, **597**, 418.
50 N. O. Dhoot and M. A. Wheatley, *J. Pharm. Sci*., 2003, **92**, 679.
51 T. M. Allen and J. M. Everest, *J. Pharmacol. Exp. Therap*., 1983, **226**, 539.
52 X. Guo and F. C. Jr Szoka, *Bioconjug. Chem*., 2001, **12**, 291.
53 J. Ropponen, S. Nummelin and K. Rissanen, *Org. Lett*., 2004, **6**, 2495.
54 M. R. Mozafari, *Cell. Mol. Biol. Lett.,* 2005, **10**, 711.
55 E. Terreno, A. Sanino, C. Carrera, D. D. Castelli, G. B. Giovenzana, A. Lombardi, R. Mazzon, L. Milone, M. Visigalli and S. Aime, *J. Inorg. Biochem*., 2008, **102**, 1112.
56 C. Cabella,S. G. Crich,D. Corpillo, A. Barge, C. Ghirelli, E. Bruno, V. Lorusso, F. Uggeri and S. Aime, *Contrast Media Mol. Imag*., 2006, **1**, 23.
57 B. M. Mitruka and H. M. Rawnsley, Clinical Biochemical and Haematological Reference Values in Normal Experimental Animals and Normal Humans, Mosby, New York, USA **1981**.